arXiv:1602.06976v1 [cond-mat.supr-con] 22 Feb 2016

Nodal superconducting gap structure in the quasi-one-dimensional $Cs_2Cr_3As_3$ investigated using μSR measurements

D. T. Adroja,[1,2,*] A. Bhattacharyya,[1,2,3] M. Smidman,[4] A. D. Hillier,[1] Yu. Feng,[5] B. Pan,[5] J. Zhao,[5] M. R. Lees,[6] A. M. Strydom,[2] and P. K. Biswas[1]

[1]*ISIS Facility, Rutherford Appleton Laboratory, Chilton, Didcot Oxon, OX11 0QX, United Kingdom*
[2]*Highly Correlated Matter Research Group, Physics Department, University of Johannesburg, PO Box 524, Auckland Park 2006, South Africa*
[3]*Department of Physics, Ramakrishna Mission Vivekananda University, Howrah-711202, India*
[4]*Center for Correlated Matter and Department of Physics, Zhejiang University, Hangzhou 310058, China*
[5]*State Key Laboratory of Surface Physics and Department of Physics, Fudan University, Shanghai 200433, China*
[6]*Department of Physics, University of Warwick, Coventry, CV4 7AL, United Kingdom*

(Dated: February 24, 2016)

The superconducting ground state of the newly discovered superconductor $Cs_2Cr_3As_3$ with a quasi-one-dimensional crystal structure ($T_c \sim 2.1(1)$ K) has been investigated using magnetization and muon-spin relaxation or rotation (μSR), both zero-field (ZF) and transverse-field (TF), measurements. Our ZF μSR measurements reveal the presence of spin fluctuations below 4 K and the ZF relaxation rate (λ) shows enhancement below $T_c \sim 2.1$ K, which might indicate that the superconducting state is unconventional. This observation suggests that the electrons are paired via unconventional channels such as spin fluctuations, as proposed on the basis of theoretical models. Our analysis of the TF μSR results shows that the temperature dependence of the superfluid density is fitted better with a nodal gap structure than an isotropic s-wave model for the superconducting gap. The observation of a nodal gap in $Cs_2Cr_3As_3$ is consistent with that observed in the isostructural $K_2Cr_3As_3$ compound through TF μSR measurements. Furthermore, from our TF μSR study we have estimated the magnetic penetration depth $\lambda_L(0) = 954$ nm, superconducting carrier density $n_s = 4.98 \times 10^{26}$ m^{-3}, and carrier's effective-mass enhancement $m^* = 1.61m_e$.

PACS numbers: 74.70.Xa, 74.25.Op, 75.40.Cx

In a conventional superconductor, the binding of electrons into the paired states, known as the Cooper pairs, that collectively carry the supercurrent is mediated by lattice vibrations or phonons, which is the fundamental principle of the Bardeen-Cooper-Schrieffer (BCS) theory [1]. The BCS theory often fails to describe the SC observed in strongly correlated materials. Several strongly correlated superconducting materials, having magnetic $f-$ or $d-$ electron elements, exhibit unconventional SC and various theoretical models based on magnetic interactions (magnetic glue) and spin fluctuations have been proposed to understand these superconductors [2]. The superconducting gap structure of strongly correlated $f-$ and $d-$ electron superconductors is very important in understanding the physics of unconventional pairing mechanism in this class of materials.

Unconventional superconductivity has been observed in high-temperature cuprates [3], iron pnictides [4] and heavy fermion materials [5], which have strong electronic correlations and quasi two dimensionality. It is of great interest to explore possible unconventional SC in a quasi-one-dimensional Q1D material with significant electron correlations. The recently discovered superconductors with a Q1D crystal structure, $K_2Cr_3As_3$ $T_c \sim 6.1$ K, $Rb_2Cr_3As_3$ $T_c \sim 4.8$ K and $Cs_2Cr_3As_3$ $T_c \sim 2.2$ K have been intensively investigated both experimentally and theoretically [6–16] as they are strong candidates for a multiband triplet pairing state as well as spin fluctuation mediated superconductivity from the d-electrons of the Cr ions. In recent years the search for triplet superconductivity has been one of the major research efforts partly due to its intrinsic connection to topologically related physics and quantum computation. These new superconductors are conjectured to possess an unconventional pairing mechanism [6, 9–13]. There are several pieces of experimental evidence for this. Firstly, the upper critical field H_{c2} perpendicular to Cr-chain is significantly larger than the Pauli limit, but parallel to the Cr-chain it exhibits a paramagnetically limited behavior, indicating that the BCS-type pairing is unfavorable [7, 17–19]. Secondly, strong electronic correlations which are a common feature of unconventional superconductivity were revealed by a large electronic specific heat coefficient and non-Fermi liquid transport behavior [6, 19]. This is consistent with the the Q1D crystalline structure of $A_2Cr_3As_3$ (A = K, Rb and Cs) and represents a possible realization of a Luttinger liquid state [20]. Thirdly, line nodal gap symmetry was revealed by London penetration depth and superfluid density measurements of $K_2Cr_3As_3$ [10, 11]. Fourthly, the effect of nonmagnetic impurities reveals that the T_c decreases significantly for $K_2Cr_3As_3$ [21], in accordance with the general-

*Electronic address: devashibhai.adroja@stfc.ac.uk

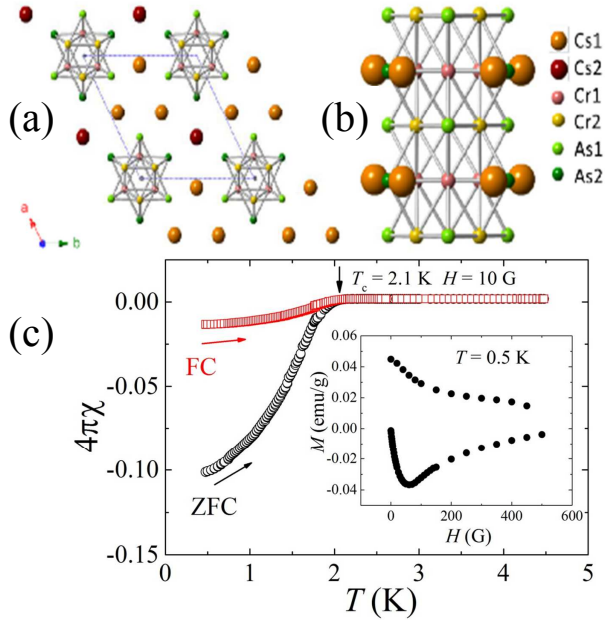

FIG. 1: (Color online) (a) The quasi-1D crystal structure of $Cs_2Cr_3As_3$ and (b) the c-axis view of the crystal structure showing $[Cr_3As_3]_\infty$ chain. (c) The temperature dependence of the dc magnetic susceptibility measured in zero-field cooled state (ZFC) and field cooled state (FC) of $Cs_2Cr_3As_3$ in the presence of an applied magnetic field of 10 G. The inset in (c) shows the magnetization versus field at 0.5 K.

ized Abrikosov-Gorkov pair-breaking theory, which supports a non-s-wave superconductivity.

Theoretically, by using density functional theory (DFT) calculations, X. Wu *et al.* predicted $K_2Cr_3As_3$ to be near a novel in-out co-planar magnetically ordered state and possess strong spin fluctuations [12, 13]. Furthermore, it has been shown that a minimum three-band model based on the d_{z^2} , d_{xy} and $d_{x^2-y^2}$ orbitals of one Cr sublattice can capture the band structure near the Fermi surfaces. First principle calculations for $K_2Cr_3As_3$ reveal that one three-dimensional Fermi surface and two quasi-one-dimensional Fermi sheets cross the Fermi energy [22–24]. In both the weak and strong coupling limits, the standard random phase approximation (RPA) and mean-field solutions consistently yield a triplet p_z-wave pairing as the leading pairing symmetry for physically realistic parameters [12, 25–28]. The triplet pairing is driven by ferromagnetic fluctuations within the sublattice [12, 13, 22]. The gap function of the pairing state possesses line gap nodes on the $k_z = 0$ plane of the Fermi surface. So it is highly likely that electrons are paired via unconventional channels such as spin fluctuations in $A_2Cr_3As_3$. Nuclear magnetic resonance (NMR) and nuclear quadrupole resonance (NQR) measurements indeed reveal the enhancement of spin fluctuations approaching T_c in $K_2Cr_3As_3$ [20] and $Rb_2Cr_3As_3$ [29]. Furthermore Y. Zhou *et al.* [28] have shown theoretically that at small Hubbard U and moderate Hund's coupling, the pairing arises from the 3-dimensional (3D) γ band and has $f_{y(3x^2-y^2)}$ symmetry, which gives line nodes in the gap function. At large U, a fully gapped p-wave state dominates on the quasi-1D α-band. There are large numbers of experimental results as well as theoretical calculations reported on $A_2Cr_3As_3$ (A = K and Rb), however, not much experimental work has been reported on $Cs_2Cr_3As_3$. This is due to the difficulties in synthesizing samples of this material, because of its high air sensitivity [8]. We have been able to synthesize good quality powder sample of $Cs_2Cr_3As_3$ and have investigated this material using magnetization and μSR measurements.

A polycrystalline sample of $Cs_2Cr_3As_3$ was prepared as described by Tang *et al.* [8]. This sample was characterized using x-ray diffraction and magnetic susceptibility. The magnetization data were measured using a Quantum Design Superconducting Quantum Interference Device magnetometer equipped with an iQuantum He-3 insert between 0.4 and 4.5 K. Muon spin relaxation/rotation (μSR) experiments were carried out on the MUSR spectrometer at the ISIS pulsed muon source of the Rutherford Appleton Laboratory, UK [30]. The μSR measurements were performed in zero−field (ZF), and transverse−field (TF) mode. A polycrystalline sample of $Cs_2Cr_3As_3$ was mounted in a sealed titanium (99.99%) sample holder under He-exchange gas, which was placed in a dilution refrigerator operating in the temperature range of 50 mK−5 K. It should be noted that we used small pieces of the sample, (not fine powder), to minimize the decomposition of the sample, as the sample is very air sensitive. Using an active compensation system the stray magnetic fields at the sample position were canceled to a level of 1 mG. TF−μSR experiments were performed in the superconducting mixed state in an applied field of 400 G, well above the lower critical field of H_{c1}= 10 G of this material. Data were collected in the (a) field−cooled (FC) mode, where the magnetic field was applied above the superconducting transition and the sample was then cooled down to base temperature and (b) zero field cooled (ZFC) mode, where first the sample was cooled down to 0.05 K in ZF and then the magnetic field was applied. Muon spin relaxation is a dynamic method that allows one to resolve the nature of the pairing symmetry in superconductors [31]. The mixed or vortex state in the case of type-II superconductors gives rise to a spatial distribution of local magnetic fields; which demonstrates itself in the μSR signal through a relaxation of the muon polarization. The asymmetry of the muon decay in ZF is calculated by, $G_z(t) = [N_F(t) - \alpha N_B(t)]/[N_F(t) + \alpha N_B(t)]$, where $N_F(t)$ and $N_B(t)$ are the number of counts at the detectors in the forward and backward positions respectively and α is a constant determined from calibration measurements made in the paramagnetic state with a small (20 G) applied transverse magnetic field. The data were

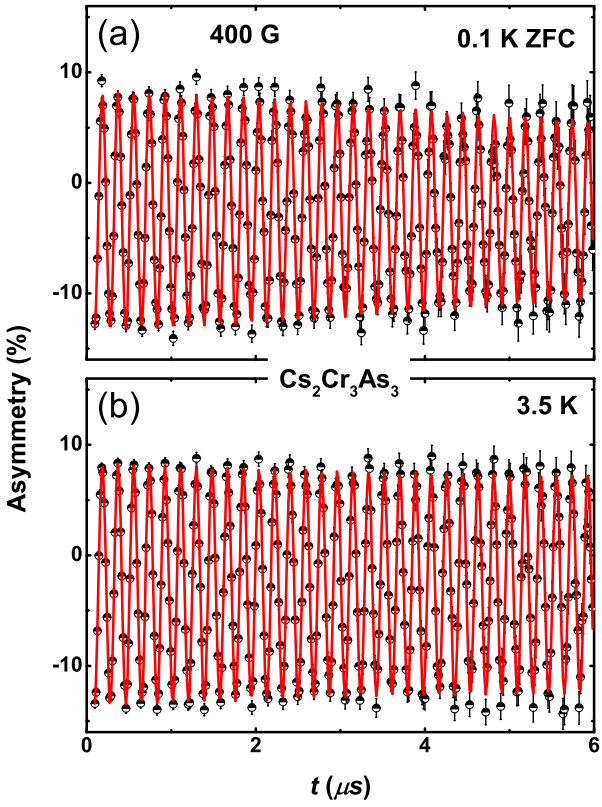

FIG. 2: (Color online) The transverse-field μSR time spectra (one component) for $Cs_2Cr_3As_3$ collected (a) at $T = 0.1$ K and (b) at $T = 3.5$ K in an applied magnetic field $H = 400$ G for the zero-field cool (ZFC) state.

analyzed using the free software package WiMDA [32].

The analysis of the x-ray powder diffraction at 300 K reveals that the sample is single phase and crystallizes with space group $P\bar{6}m2$ (No. 187). The hexagonal crystal structure of $Cs_2Cr_3As_3$ is shown in Figs. 1(a-b). The Q1D feature of $Cs_2Cr_3As_3$ is manifested by the chains of $[Cr_3As_3]_\infty$ octahedra (or double-walled subnanotubes) running along the c direction (Fig.1b). which are separated by columns of Cs^+ ions, in contrast to the layered iron-pnictide and copper-oxide high T_c superconductors. Magnetic susceptibility measurements in an applied field of 10 G show superconductivity occurs at 2.1(1) K and the superconducting volume fraction is close to 10% at 0.5 K (Fig. 1(c)), indicating the bulk nature of superconductivity in $Cs_2Cr_3As_3$. The small volume fraction of the superconductivity observed in our sample through the magnetic susceptibility measurements is in agreement with only 6% superconducting volume fraction reported in the first report by Tang *et al.* [8]. Another possible reason for a small SC volume fraction observed in our magnetic susceptibility measurements is that these measurements were carried out three months after our μSR study and it is likely that the sample partially decomposed during this time. The magnetization isotherm $M(H)$ curve at 0.5 K (inset of Fig.1(c)) shows a typical behaviour for type-II superconductivity. We have estimated the lower critical field (H_{c1}) of 10 G from the initial deviation from the linear behavior. The reported value of the upper critical field H_{c2}=64.5 kG [8] is higher than the Pauli limit, $\mu_0 H_P = 18.4 T_c = 38.64$ kG [17], indicating unconventional superconductivity. In zero field, the temperature-dependent resistivity of $Cs_2Cr_3As_3$ is metallic [8] and exhibits linear temperature dependence between 50 K and just above T_c, indicating non-Fermi-liquid behavior and suggesting the importance of spin fluctuations [8]. At the superconducting transition, the dimensionless specific heat jump is $\Delta C/\gamma\ T_c = 0.4$, which is smaller than the simple $s-$wave BCS prediction 1.43 [8]. The smaller value of the observed jump in the heat capacity was attributed to degradation of the sample [8].

Figures 2 (a) and (b) show the TF$-\mu$SR precession signals above and below T_c obtained in ZFC mode with an applied field of 400 G (well above $H_{c1} \sim 10$ G but below $H_{c2} \sim 64.5$ kG). The observed decay of the μSR signal with time below T_c is due to the inhomogeneous field distribution of the flux-line lattice. We have used an oscillatory decaying Gaussian function to fit the TF$-\mu$SR asymmetry spectra, which is given below,

$$G_{z1}(t) = A_1 \cos(2\pi\nu_1 t + \phi_1) \exp\left(\frac{-\sigma^2 t^2}{2}\right) + A_2 \cos(2\pi\nu_2 t + \phi_2), \quad (1)$$

where ν_1 and ν_2 are the frequencies of the muon precession signal from the sample and from the background signal from the Ti-sample holder, respectively, ϕ_i ($i = 1, 2$) are the initial phase offsets. A_1 and A_2 are the muon initial asymmetries associated with the sample and background (from the Ti-sample holder), respectively. The fits reveal the relative values of $A_1 = 35\%$ and $A_2 = 65\%$. It is noted that the value of A_2 is higher than A_1. The reason for this is that the muons have to first pass through the titanium foil (30 μm thick) and then stop in the sample. Another reason for the large background asymmetry is due to the fact that we have used small pieces of the sample rather than fine powder to minimize the decomposition of the sample and hence it is possible that pieces might have settled down at the bottom of the sample holder when mounted vertically on the instrument. This also results in a higher fraction of the muons stopping directly in the titanium sample holder. Furthermore, the sample is very air sensitive and some parts of the sample may have decomposed. In Eq. 1 the first term contains the total sample relaxation rate σ; there are contributions from both the vortex lattice (σ_{sc}) and nuclear dipole moments (σ_{nm}), which is assumed to be constant over the entire temperature range below T_c [where $\sigma = \sqrt{(\sigma_{sc}^2 + \sigma_{nm}^2)}$]. The contribution from the

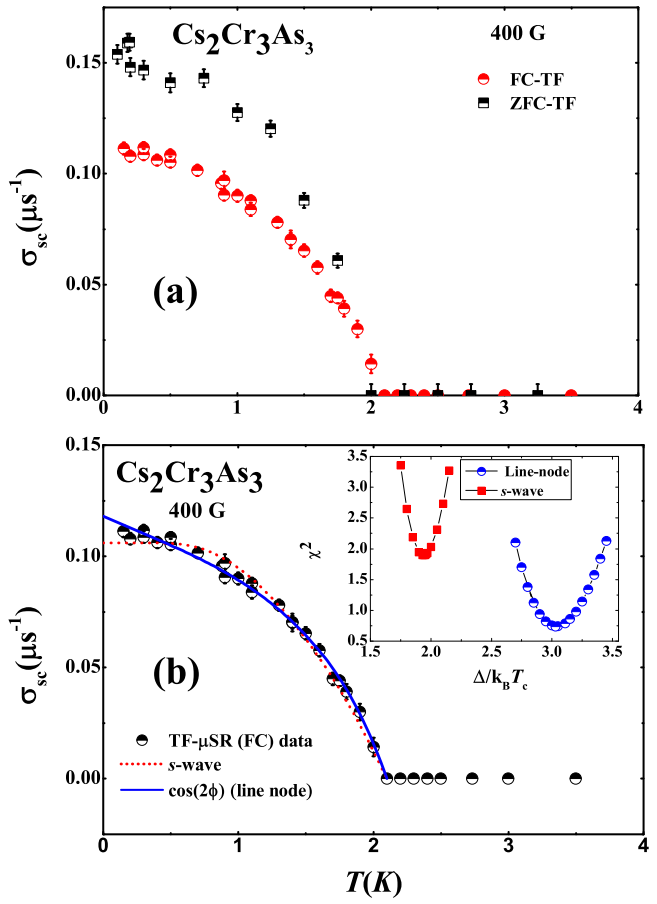

FIG. 3: (Color online) (a) The temperature dependence of muon depolarization rate $\sigma_{sc}(T)$ of $Cs_2Cr_3As_3$ collected in an applied magnetic field of 400 G in zero-field cooled (ZFC) and field cooled (FC) modes. (b) $\sigma_{sc}(T)$ of FC mode (symbols) and the lines are the fits to the data using Eq. 2. The short-dashed red line shows the fit using an isotropic single-gap s-wave model with $\Delta_0/k_B/T_c = 1.94\pm0.01$ and the solid blue line shows the fit to a nodal gap model with $\Delta_0/k_BT_c = 3.0\pm0.2$, respectively. The inset shows the plot of quality of fit χ^2 versus $\Delta_0/k_B/T_c$.

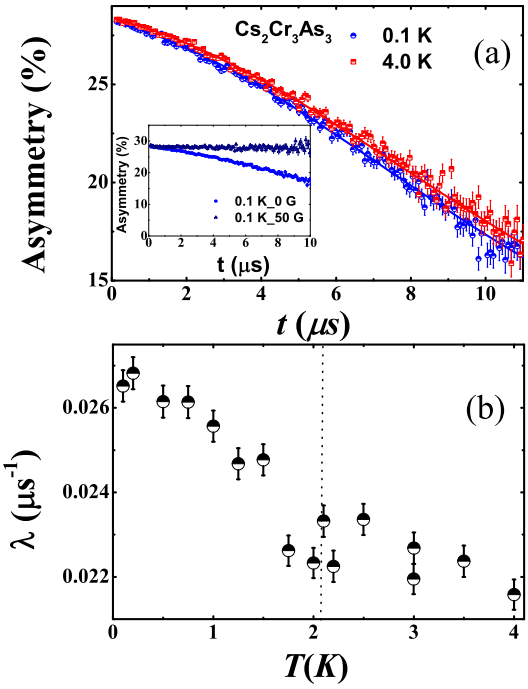

FIG. 4: (Color online) (a) Zero-field μSR time spectra for $Cs_2Cr_3As_3$ collected at 0.1 K (blue circle) and 4.0 K (red square) are shown together with lines that are least squares fits to the data using Eq. (3). (b) The temperature dependence of the electronic relaxation rate measured in zero magnetic field of $Cs_2Cr_3As_3$, where $T_c = 2.1$ K is shown by the vertical dotted line. The inset in (a) shows the spectra measured in 50 G longitudinal field together with ZF field results for comparison.

vortex lattice, σ_{sc}, was determined by quadratically subtracting the background nuclear dipolar relaxation rate obtained from the spectra measured above T_c. As σ_{sc} is directly related to the superfluid density, it can be modeled by [33]

$$\frac{\sigma_{sc}(T)}{\sigma_{sc}(0)} = 1 + 2\left\langle \int_{\Delta_k}^{\infty} \frac{\partial f}{\partial E} \frac{E\mathrm{d}E}{\sqrt{E^2-\Delta_k^2}} \right\rangle_{\mathrm{FS}}, \qquad (2)$$

where $f = [1+\exp(-E/k_BT)]^{-1}$ is the Fermi function and the brackets correspond to an average over the Fermi surface. The gap is given by $\Delta(T,\varphi)=\Delta_0\delta(T/T_c)g(\varphi)$, where φ is the azimuthal angle along the Fermi surface. At present, no reliable experimental value of the $\Delta C/\gamma T_c$ is available for $Cs_2Cr_3As_3$, we therefore have used the BCS formula for the temperature dependence of the gap, which is given by $\delta(T/T_c)$ =tanh$[(1.82)(1.018(T_c/T-1))^{0.51}]$ [33, 34], with g(φ) = 1 for the s-wave model and g(φ)=$|\cos(2\varphi)|$ for the d-wave model with line nodes [33, 34].

Fig. 3 (a) shows the T dependence of σ_{sc}, measured in an applied field of 400 G collected in two different modes: zero-field-cooled (ZFC) and field cooled (FC). The temperature dependence of σ_{sc} increases with decreasing temperature confirming the presence of a flux-line lattice and indicates a decrease of the magnetic penetration depth with decreasing temperature. Comparing the ZFC and FC data reveals a substantial difference. In the ZFC mode, σ_{sc} increases with decreasing temperature faster than for the FC data and thus points to differences in the number of the pinning sites, and trapping energies which are altered by magnetic field history of the sample. From the analysis of observed temperature dependence of σ_{sc}, using different models, the nature of the superconducting gap can be determined. We have analyzed the temperature dependence of σ_{sc} based on two models: an isotropic s-wave gap model and a line nodes model. The fit to $\sigma_{sc}(T)$ data of $Cs_2Cr_3As_3$ by a single isotropic s-wave gap using Eq.(2) gives $\Delta_0/k_B/T_c =$

1.94 ± 0.01 and $\sigma_{sc}(0) = 0.106 \pm 0.001$ μs^{-1} with the goodness of the fit $\chi^2 = 1.94$ (see Fig. 3b, red short-dashed line). The fit to the nodal model (blue solid line Fig. 3b) shows better agreement than that of s-wave model and gives a larger value of $\Delta_0/k_B T_{\mathbf{c}} = 3.0 \pm 0.2$ and $\sigma_{sc}(0) = 0.118 \pm 0.002$ μs^{-1} with $\chi^2 = 0.75$. We also tried s-wave and nodal d-wave fits with various fixed values of $\Delta_0/k_B T_{\mathbf{c}}$ and allowing only $\sigma_{sc}(0)$ to vary, to compare the (χ^2) values between these two models (see the inset in Fig. 3b). These plots of χ^2 confirms that our data fit better to the nodal gap model than the isotropic gap s-wave model. Therefore our μSR analysis is more consistent with $Cs_2Cr_3As_3$ having line nodes than being fully gapped. This is in agreement with the μSR results of $K_2Cr_3As_3$ [11], which also support the presence of line nodes in the superconducting gap.

Furthermore, the large value of $\Delta_0/k_B/T_c = 3.0 \pm 0.2$ obtained from the line nodes d-wave fit is larger than the 1.764 expected for BCS superconductors, indicates the presence of strong coupling and unconventional superconductivity, which is in line with that observed in $K_2Cr_3As_3$ $\Delta_0/k_B/T_c = 3.2 \pm 0.1$ [11]. In addition, a ^{75}As NMR study on $K_2Cr_3As_3$ and $Rb_2Cr_3As_3$ reveals the absence of a Hebel-Slichter coherence peak of $1/T_1$ just below $T_{\mathbf{c}}$, which is followed by a steep decrease, in analogy with unconventional superconductors in higher dimensions with point or line nodes in the energy gap [20, 29]. Furthermore, the T^5 variation of the spin-lattice relaxation rate $1/T_1$ at low temperatures in $Rb_2Cr_3As_3$ suggests unconventional superconductivity with point nodes in the gap function [29]. Both the NMR Knight Shift and $1/T_1$T increase upon cooling below 100 K, which are consistent with ferromagnetic spin fluctuations in both K and Rb samples [20, 29]

The Hebel-Slichter coherence peak of $1/T_1$ is a crucial test for the validity of the description of the superconducting state based on the conventional isotropic BCS s-wave model. The absence of the coherence peak in $1/T_1$ of $A_2Cr_3As_3$ (A = K and Rb) suggests that an isotropic s-wave model is not an appropriate model to explain the gap symmetry. These results along with our μSR analysis of $Rb_2Cr_3As_3$ and $Cs_2Cr_3As_3$ suggest that a nodal gap in all three compounds.

The muon spin depolarization rate (σ_{sc}) below $T_{\mathbf{c}}$ is related to the magnetic penetration depth (λ). For a triangular lattice, [35–37] $\frac{\sigma_{sc}(T)^2}{\gamma_\mu^2} = \frac{0.00371\phi_0^2}{\lambda^4(T)}$, where $\gamma_\mu/2\pi = 135.5$ MHz/T is the muon gyromagnetic ratio and $\phi_0 = 2.07\times10^{-15}$ T m^2 is the flux quantum. As with other phenomenological parameters characterizing a superconducting state, the penetration depth can also be related to microscopic quantities. Using London theory [35], $\lambda_L^2 = m^* c^2/4\pi n_s e^2$, where $m^* = (1 + \lambda_{e-ph})m_e$ is the effective mass and n_s is the density of superconducting carriers. Within this simple picture, λ_L is independent of magnetic field. λ_{e-ph} is the electron-phonon coupling constant, which can be estimated from Θ_D and T_c using McMillan's relation [38] $\lambda_{e-ph} = \frac{1.04+\mu^* \ln(\Theta_D/1.45T_c)}{(1-0.62\mu^*)\ln(\Theta_D/1.45T_c)+1.04}$, where μ^* is the repulsive screened Coulomb parameter usually assigned as $\mu^* = 0.13$. For $Cs_2Cr_3As_3$ we have used $T_{\mathbf{c}} = 2.1$ K and $\Theta_D = 160$ K , which together with $\mu^* = 0.13$, we have estimated $\lambda_{e-ph} = 0.75$. Further assuming that roughly all the normal state carriers (n_e) contribute to the superconductivity (i.e., $n_s \approx n_e$), we have estimated the magnetic penetration depth λ, superconducting carrier density n_s, and effective-mass enhancement m^* to be $\lambda_L(0) = 954(9)$ nm (from the nodal fit), $n_s = 4.98\times10^{26}$ carriers/m^3, and $m^* = 1.61\ m_e$, respectively. More details on these calculations can be found in Refs. [39–41]. Very similar value of n_s and m^* were estimated for $K_2Cr_3As_3$, but the $\lambda_L(0)$= 432 nm was a factor 2.2 smaller [11].

The measured ZF$-\mu$SR spectra of $Cs_2Cr_3As_3$ are shown in Fig. 4(a) for $T = 0.1$ and 4.0 K. In ZF relaxation experiments, any muons stopping in the titanium sample holder give a time independent background. The absence of a muon precession signal in the spectra in Fig. 4(a), rules out the presence of a long-range magnetic ordered ground state in this compound. One possibility is that the muon−spin relaxation is due to either static, randomly oriented local fields associated with the nuclear moments at the muon site or the fluctuating electronic moments. The ZF$-\mu$SR data are well described by,

$$G_{z2}(t) = A_1 e^{-\lambda t} + A_{bg} \tag{3}$$

where λ is the electronic relaxation rate, A_1 is the initial asymmetry and A_{bg} is the background. The parameters A_1, and A_{bg} are found to be temperature independent. It is interesting to note that λ is finite at 4 K and increases [Fig. 4 (b)] with an onset temperature of $\geq 2.1 \pm 0.1$ K, indicating slowing down of electronic spin fluctuations correlated with the superconductivity. This observation suggests that the superconductivity of $Cs_2Cr_3As_3$ is most probably associated with the spin fluctuation mechanism, which is supported by the NMR and NQR measurements on $A_2Cr_3As_3$ (A = K and Rb) [20, 29]. The increases in λ at T_c has been observed in superconducting state of Sr_2RuO_4 [42], $LaNiC_2$ [43], $Lu_5Rh_6Sn_{18}$ [44] and $Y_5Rh_6Sn_{18}$ [45], but above T_c λ remains almost constant in these compounds. This type of increase in λ has been explained in terms of a signature of a coherent internal field with a very low frequency associated with time reversal symmetry (TRS) breaking by Luke *et al.* [42] for Sr_2RuO_4. Therefore based on these observations and considering the temperature dependence of λ above and below T_c in $Cs_2Cr_3As_3$, we suggest that spin fluctuations play an important role in the superconductivity. A very similar temperature dependent behavior of the ZF μSR depolarization rate is observed above and below the superconducting transition in RRuB$_2$ (R =

Lu, Y) by Barker *et al.* [46], which has been attributed to the presence of quasistatic magnetic fluctuations.

In summary, we have presented zero-field (ZF) and transverse field (TF) muon spin rotation (μSR) measurements in the normal and the superconducting state of $Cs_2Cr_3As_3$, which has a quasi-one-dimensional crystal structure. Our ZF μSR data reveal the presence of spin fluctuations at 4 K, which become stronger passing through the superconducting transition $T_c = 2.1$ K, indicating that the spin fluctuations are important for the superconducting state. The change of the ZF relaxation rate $\Delta\lambda$ from 4 K (i.e above T_c) to the lowest temperature is $5 \times 10^{-3}\mu s^{-1}$ in $Cs_2Cr_3As_3$, which is a factor of 20 larger than that observed in $K_2Cr_3As_3$ ($\Delta\lambda = 2.5 \times 10^{-4}\mu s^{-1}$) despite the fact that the ratio of T_c is 0.34. Considering Cs is a larger ion than K we would expect the lattice expansion to lead to reduction in the spin fluctuations in $Cs_2Cr_3As_3$ when compared to $K_2Cr_3As_3$, which is not the case and hence remains to be understood. From the TF μSR we have determined the muon depolarization rate in ZFC and FC modes associated with the vortex-lattice. The temperature dependence of σ_{sc} fits better to a nodal gap model than an isotropic $s-$wave model. Further, the value of $\Delta_0/k_B/T_c = 3.0\pm0.2$ obtained from the nodal gap model fit is larger than the 1.764 expected for BCS superconductors, indicating the presence of strong coupling and unconventional superconductivity in $Cs_2Cr_3As_3$. These results are in agreement with our previous finding for $K_2Cr_3As_3$. Considering the possibility of multi-band nature of superconductivity in $A_2Cr_3As_3$ (A = K, Rb and Cs) one would expect more complex behavior of the gap function and hence the conclusions obtained from our TF μSR study are in line with this. Further confirmation of the presence of line nodes in the superconducting gap requires μSR, heat capacity and thermal conductivity investigations of good quality single crystals of $Cs_2Cr_3As_3$.

DTA and ADH would like to thank CMPC-STFC, grant number CMPC-09108, for financial support. A.B would like to acknowledge FRC of UJ, NRF of South Africa and ISIS-STFC for funding support. Work at Fudan University is supported by the Shanghai Pujiang Scholar Program (Grant No.13PJ1401100). AMS thanks the SA-NRF (Grant 93549) and UJ Research Committee for financial support.

[1] J. Bardeen, L. N. Cooper, and J. R. Schrieffer, Phys. Rev. **106**, 162 (1957).
[2] J. Paglione and R. L. Greene, Nature Physics. **6**, 642 (2010).
[3] P. Dai, H. A. Mook, S. M. Hayden, G. Aeppli, T. G. Perring, R. D. Hunt, and F. Dogan, Science. **284**, 1344 (1999).
[4] P. Dai, Rev. Mod. Phys. **87**, 855 (2015).
[5] M. P. Allan, F. Massee, D. K. Morr, J. Van Dyke, A.W. Rost, A. P. Mackenzie, C. Petrovic and J. C. Davis, Nature Physics. **9**, 468 (2013).
[6] J.-K. Bao, J.-Y. Liu, C.-W. Ma, Z.-H. Meng, Z.-T. Tang, Y.-L. Sun, H.-F. Zhai, H. Jiang, H. Bai, C.-M. Feng, Z.-A. Xu, and G.-H. Cao, Phys. Rev. X **5**, 011013 (2015).
[7] T. Kong, S. L. Budko, and P. C. Canfield, Phys. Rev. B **91**, 020507(R) (2015).
[8] Z.-T. Tang, J.-K. Bao, Z. Wang, H. Bai, H. Jiang, Y. Liu, H.-F. Zhai, C.-M. Feng, Z.-A. Xu, G.-H. Cao, Science China Materials, **58**, 16 (2015).
[9] Z.-T. Tang, J.-K. Bao, Y. Liu, Y.-L. Sun, A. Abliit, H.-F. Zhai, H. Jiang, C.-M. Feng, Z.-A. Xu, and G.-H. Cao, Phys. Rev. B **91**, 020506(R), (2015).
[10] G. M. Pang, M. Smidman, W. B. Jiang, J. K. Bao, Z. F. Weng, Y. F. Wang, L. Jiao, J. L. Zhang, G. H. Cao and H. Q. Yuan, Phys. Rev. B **91**, 220502(R) (2015).
[11] D. T. Adroja, A. Bhattacharyya, M. Telling, Yu. Feng, M. Smidman, B. Pan, J. Zhao, A. D. Hillier, F. L. Pratt, and A.M. Strydom, Phys. Rev. B **92**, 134505 (2015).
[12] X. Wu, C. Le, J. Yuan, H. Fan and J. Hu, Chin. Phys. Lett. **32**, 057401 (2015).
[13] H. Zhong, X. Y. Feng, H. Chen, J. Dai, Phys. Rev. Lett. **115**, 227001 (2015).
[14] G. M. Pang, M. Smidman, Y. G. Jiang, Shi, W. B., J. K. Bao, Z. T. Tang, Z. F. Weng, Y. F. Wang, L. Jiao, J. L. Zhang, J. L. Luo, G. H. Cao, and H. Q. Yuan, J. Magn. Magn. Mater., **84**, 400 (2016).
[15] L-D. Zhang, X. Wu, H. Fan, F. Yang and J. Hu, arXiv:1512.00147.
[16] C. Cao, H. Jiang, X.-Y. Feng, and J. Dai, Phys. Rev. B **92**, 235107 (2015)
[17] A. M. Clogston, Phys Rev Lett, **9**, 266 (1962).
[18] F. Balakirev, T. Kong, M. Jaime, R. D. McDonald, C. H. Mielke, A. Gurevich, P. C. Canfield, and S. L. Budko, Phys. Rev. B **91**, 220505(R) (2015)
[19] X. F. Wang, C. Roncaioli, C. Eckberg, H. Kim, J. Yong,Y. Nakajima, S. R. Saha, P.Y. Zavalij, and J. Paglione, Phys. Rev. B **92**, 020508(R) (2015)
[20] H. Z. Zhi, T. Imai, F. L. Ning, J.-K. Bao, and G.-H. Cao, Phys. Rev. Lett. **114**, 147004 (2015).
[21] Y. Liu, J. K. Bao, H. K. Zuo, A. Ablimit, Z. T. Tang, C. M. Feng, Z. W. Zhu, and G. H. Cao, Sci. China-Phys. Mech. Astron. **59**, 657402 (2016).
[22] H. Jiang, G. Cao, and C. Cao, Scientific Reports **5**, 16054 (2015).
[23] P. Alemany and E. Canadell, Inorganic Chemistry **54**, 8029 (2015).
[24] A. Subedi, Phys. Rev. B, **92**, 174501 (2015).
[25] X. Wu, F. Yang, S. Qin, H. Fan and J. Hu, Phys. Rev. B **92**, 104511 (2015).
[26] X. Wu, F, Yang, C. Le, H. Fan and J. Hu, Phys. Rev. B **92**, 104511 (2015).
[27] H. Zhong, X.-Y. Feng, H. Chen, and J. Dai, Phys. Rev. Lett., **115**, 227001 (2015).
[28] Y. Zhou, C. Cao, and F.-C. Zhang, arXiv1502.03928v2.
[29] J. Yang, Z. T. Tang, G. H. Cao, and Guo-qing Zhen, Phys. Rev. Lett., **115**, 147002 (2015).
[30] S. L. Lee, S. H. Kilcoyne, and R. Cywinski, *Muon Science: Muons in Physics, Chemistry and Materials* (SUSSP Publications and IOP Publishing, Bristol, 1999).
[31] J. E. Sonier, J. H. Brewer, and R. F. Kiefl, Rev. Mod. Phys. **72**, 769 (2000).

[32] F.L. Pratt, Physica B **289-290**, 710 (2000).
[33] R. Prozorov, and R. W. Giannetta, Supercond. Sci. Technol. **19**, R41 (2006).
[34] A. Carrington, and F. Manzano, Physica C **385**, 205 (2003)
[35] See, for example, J. E. Sonier, J. H. Brewer, and R. F. Kiefl, Rev. Mod. Phys. **72**, 769 (2000).
[36] See, for example, A. Amato, Rev. Mod. Phys. **69**, 1119 (1997).
[37] E. E. M. Chia, M. B. Salamon, H. Sugawara, and H. Sato, Phys. Rev. B **69**, 180509(R) (2004).
[38] W. McMillan, Phys. Rev. **167**, 331 (1968).
[39] A. D. Hillier and R. Cywinski, Appl. Magn. Reson. **13**, 95 (1997).
[40] V. K. Anand, D. Britz, A. Bhattacharyya, D. T. Adroja, A. D. Hillier, A. M. Strydom, W. Kockelmann, B. D. Rainford, and K. A. McEwen, Phys. Rev. B **90**, 014513 (2014).
[41] D. T. Adroja, A. D. Hillier, J. -G. Park, E. A. Goremychkin, K. A. McEwen, N. Takeda, R. Osborn, B. D. Rainford, and R. M. Ibberson, Phys. Rev. B **72**, 184503 (2005).
[42] G. M. Luke, Y. Fudamoto, K. M. Kojima, M. I. Larkin, J. Merrin, B. Nachumi, Y. J. Uemura, Y. Maeno, Z. Q. Mao, Y. Mori et al., Nature (London) **394**, 558 (1998).
[43] A. D. Hillier, J. Quintanilla, and R. Cywinski, Phys. Rev. Lett. **102**, 117007 (2009).
[44] A. Bhattacharyya, D.T. Adroja, J. Quintanilla, A.D. Hillier, N. Kase, A.M. Strydom and J. Akimitsu, Phys. Rev. B **91**, 060503(R), (2015).
[45] A. Bhattacharyya, D.T. Adroja, N. Kase, A.D. Hillier, J. Akimitsu and A.M. Strydom, Sci. Rep. **5**, 12926 (2015).
[46] J. A. T. Barker, R. P. Singh, A. D. Hillier, and D. McK. Paul, arXiv:1508.00486v1